

magnitude, will depend on the detailed form of the low-energy behavior of $\alpha^2(\omega)F(\omega)$. For the theoretical calculations given here, $\alpha^2(\omega)F(\omega)$ has been chosen to be linear in ω for reasons of simplicity⁷; the choice $\alpha^2(\omega)F(\omega) = \alpha^2\omega^2$ would not affect the general conclusions.

In conclusion, the observed structure near zero bias in the conductance σ and its derivative $d\sigma/dV$ for normal metal-insulator-metal tunneling junctions has been accounted for by including the effects of finite electron relaxation rates in the junction electrodes. The nonzero lifetimes lead to an observable blocking of otherwise-available electron tunneling states at low bias.

*Work supported in part by grants from the National Research Council of Canada.

¹See, for example, the review by C. B. Duke, *Tunnel-*

ing in Solids, Suppl. 10 to *Solid State Physics*, edited by F. Seitz, D. Turnbull, and H. Ehrenreich (Academic, New York, 1969).

²J. Lambe and R. C. Jaklevic, *Phys. Rev.* **165**, 821 (1968); J. M. Rowell, W. L. McMillan, and W. L. Feldmann, *Phys. Rev.* **180**, 658 (1969).

³T. T. Chen and J. G. Adler, *Solid State Commun.* **8**, 1965 (1970).

⁴H. R. Zeller and I. Giaever, *Phys. Rev.* **181**, 789 (1969).

⁵See, for example, J. W. Wilkins, *Observable Many Body Effects in Metals* (Nordita, Copenhagen, 1968).

⁶These measurements were obtained by standard high-resolution spectroscopy methods; see, for example, J. G. Adler, T. T. Chen, and J. Straus, *Rev. Sci. Instrum.* **42**, 362 (1971).

⁷A calculation of $\alpha^2(\omega)F(\omega)$ using one orthogonalized plane wave gives a linear low-energy behavior; see, e. g., J. P. Carbotte and R. C. Dynes, *Phys. Rev.* **172**, 476 (1968). Because of band-structure effects it is not expected that $\alpha^2(\omega)F(\omega)$ remains linear in the very low-energy region. We have used $\alpha^2 = 3 \times 10^{-3} \text{ meV}^{-1}$.

Magnetoplasma Surface Waves in Polar Semiconductors: Retardation Effects*

K. W. Chiu and J. J. Quinn†

Brown University, Providence, Rhode Island 02912, and Max-Planck-Institut für Festkörperforschung, Stuttgart, Germany

(Received 19 June 1972)

Full dispersion curves, including the effect of retardation, are presented for the coupled optical-phonon-magnetoplasmon surface waves of a degenerate polar semiconductor. The dispersion curves display a surprising amount of interesting new structure which does not occur in the absence of a dc magnetic field.

The effect of a dc magnetic field on the dispersion relation of surface plasmons in solids has recently received considerable theoretical attention.¹⁻³ For a completely arbitrary magnetic field, the dependence of the surface-plasmon frequency on the magnitude and orientation of the applied field has been given² for the nonretarded limit in which the phase velocity ω/q is small compared with the speed of light c . The full dispersion curve, including the effect of retardation, has been studied for particular cases in which the applied field is either parallel or perpendicular to the surface.¹ Recently, Brion *et al.*³ have re-investigated one of the cases studied in Ref. 1, that of magnetoplasma surface-wave propagation perpendicular to a dc magnetic field which is oriented parallel to the surface. They found that gaps appear in the dispersion relation if the background dielectric constant ϵ_L satisfies the inequality $\epsilon_L^2 > 1 + \epsilon_L^{-1}\omega_c^{-2}\omega_p^2$, where $\omega_p = (4\pi ne^2/m)^{1/2}$ is the bulk plasma frequency.

In all of these papers the background dielectric constant was considered to be independent of frequency. For polar semiconductors, however, the background dielectric constant is not independent of frequency, but is given by

$$\epsilon_L(\omega) = \frac{\epsilon_\infty \omega^2 - \epsilon_0 \omega_T^2}{\omega^2 - \omega_T^2}, \quad (1)$$

where ϵ_∞ and ϵ_0 are the high- and low-frequency dielectric constants, and ω_T is the transverse-optical-phonon frequency. By taking into account this frequency dependence of ϵ_L , the surface plasmons and surface optical phonons are found to couple with each other.⁴ This interaction has been the object of several recent experimental studies.⁵ In the present paper, we generalize our earlier investigations^{1,2} to include the effects of phonon coupling on the magnetoplasma surface waves. Full dispersion curves for the coupled modes, including the effect of retardation, are given for different values of the experimen-

tal parameters. The dispersion curves display a remarkable amount of structure which is not present in the absence of the dc magnetic field and which should be of great experimental interest.

In order to have a point of comparison, we review briefly the case of zero magnetic field. In that case the degenerate semiconductor can be described by the dielectric function

$$\epsilon(\omega) = \epsilon_L(\omega) - \omega^{-2}\omega_p^2. \quad (2)$$

The semiconductor occupies the space $z > 0$ of a Cartesian coordinate system; the space $z < 0$ is taken to be vacuum. We refer to the semiconductor as medium 1 and the vacuum as medium 2. Subscripts referring to each medium are introduced when they are necessary. We consider an electromagnetic disturbance of the form $\exp(i\omega t - iq_y y - iq_z z)$. Surface waves are solutions of the wave equation for which q_z is imaginary. Given the real numbers q_y and ω , then the condition

$$q_{zi}^2 = (\omega^2/c^2)\epsilon_i - q_y^2. \quad (3)$$

leads to a solution of the wave equation in the semiconductor for $i=1$ [where ϵ_1 is given by Eq. (2)] and in vacuum for $i=2$ (where $\epsilon_2=1$). Surface waves exist only in those regions of the $\omega - cq_y$ plane in which both q_{z1}^2 and q_{z2}^2 are negative; then the solutions are of the form $\exp(\pm|\alpha_i|z)$, where $\alpha_i^2 = -q_{zi}^2$. The electric and magnetic fields E_1, B_1 and E_2, B_2 associated with the surface wave are eigenvectors of the wave equation and can easily be determined. By imposing the standard electromagnetic boundary conditions⁶ at the surface we obtain the dispersion relation

$$c^2 q_y^2 = \omega^2 \epsilon(\omega) / [\epsilon(\omega) + 1]. \quad (4)$$

In Fig. 1 this equation is plotted for parameters appropriate to GaAs, with a conduction electron concentration corresponding to a value of ω_p/ω_T equal to 3.3. This concentration gives rather strong coupling between the plasmon and phonon modes. For large values of cq_y/ω_T there are two surface modes of mixed plasmon-phonon character. As q_y decreases, the lower mode approaches zero linearly, while the upper mode terminates at $\omega = \omega_T$, $cq_y = \omega_T$. The lines $\omega = cq_y$, $\alpha_1 = 0$, and $\omega = \omega_T$ are the boundaries of the region of surface propagation. For $\omega > cq_y$, q_{z2}^2 is positive, and the wave becomes a propagating electromagnetic wave in vacuum. In the shaded regions of Fig. 1, q_{z1}^2 is positive, and propagating bulk modes occur.

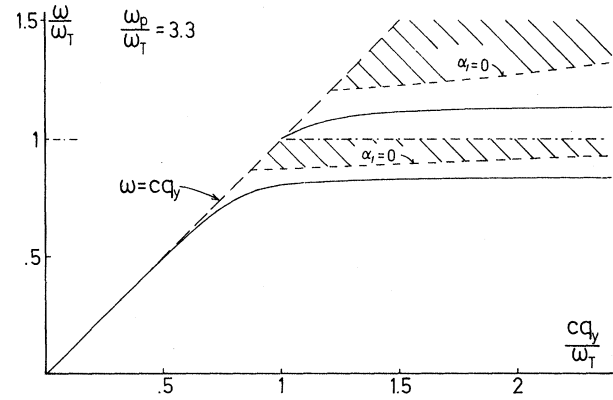


FIG. 1. A plot of ω/ω_T versus cq_y/ω_T for the case of GaAs with $\omega_p/\omega_T = 3.3$. The shaded regions and the entire region to the left of the "light line" $\omega = cq_y$ are regions in which surface-wave propagation cannot occur. The dispersion curve consists of two branches, representing the coupled surface-phonon-surface-magneton excitations.

In the presence of a dc magnetic field, the dielectric function of the semiconductor is a tensor with off-diagonal elements. For the sake of simplicity, we restrict our consideration to the case of the dc magnetic field parallel to the surface and perpendicular to the direction of propagation.^{1,3} In that case the nonvanishing components of the dielectric tensor are $\epsilon_{xx} = \epsilon_L(\omega) - \omega^{-2}\omega_p^2$, $\epsilon_{yy} = \epsilon_{zz} = \epsilon_L(\omega) - (\omega^2 - \omega_c^2)^{-1}\omega_p^2$, and $\epsilon_{yz} = -\epsilon_{zy} = -i\omega^{-1}(\omega^2 - \omega_c^2)^{-1}\omega_c\omega_p^2$. The wave equation in the semiconductor has a nontrivial solution if

$$-q_{z1}^2 = q_y^2 - (\omega^2/c^2)\epsilon_v(\omega), \quad (5)$$

where $\epsilon_v(\omega) = \epsilon_{zz} + \epsilon_{zz}^{-1}\epsilon_{yz}^2$. The wave equation in vacuum is unchanged by the magnetic field. The eigenvectors E_1, B_1 and E_2, B_2 of the wave equation can easily be determined once again. Imposing the boundary conditions leads to the dispersion relation

$$\alpha_1 + \alpha_2\epsilon_v + iq_y\epsilon_{yz}\epsilon_{zz}^{-1} = 0. \quad (6)$$

This equation is equivalent to Eq. (54) of Ref. 1 [and Eq. (7) of Ref. 3]; now, however, the diagonal components of the dielectric tensor contain the function $\epsilon_L(\omega)$ instead of the constant 1 (or the constant ϵ_∞).

In Fig. 2 we plot the solutions to Eq. (6) using parameters corresponding to the case of GaAs with $\omega_p/\omega_T = 3.3$ and $\omega_c/\omega_T = 0.4$. The dashed lines correspond to negative values of the wave number q_y , the solid line to positive values. For

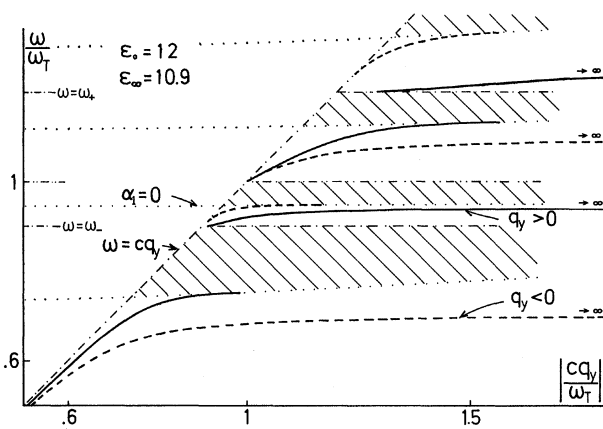


FIG. 2. A plot of ω/ω_T versus cq_y/ω_T for the case of GaAs with $\omega_p/\omega_T=3.3$ and $\omega_c/\omega_T=0.4$. The dashed and solid curves refer to negative and positive values for q_y , respectively. The shaded regions and the entire region to the left of the light line are regions in which surface-wave propagation cannot occur.

negative values of q_y , the dispersion curves are rather similar to those of Fig. 1. The lowest branch behaves linearly as $\omega = cq_y$ for very small values of cq_y/ω_T and approaches a constant for very large q_y . Another branch starts at $\omega = \omega_T$ and $cq_y = \omega_T$ and approaches a limiting value for large values of cq_y/ω_T . However, in addition to these, there are two extra branches which occur only over limited ranges of q_y . For positive q_y , both the lower branch and the upper branch (which starts at $\omega = \omega_T$) have gaps. The dispersion curves begin exactly as in the absence of the magnetic field, but they terminate at finite values of q_y ; they reappear at a higher frequency and approach their asymptotic values for very large cq_y/ω_T . For both of these branches there are regions of q_y in which two solutions exist. In the shaded region of Fig. 2, α_1^2 is negative, so that surface waves cannot occur in these regions. When a surface-wave dispersion curve has parts on both sides of one of these shaded regions, a gap in the dispersion relation must occur. The occurrence of these gaps and of the extra branches can be understood by looking at Fig. 3. Here we plot $(\omega/\omega_T)^2 \epsilon_v$ as a function of ω/ω_T . Since $\alpha_1^2 = q_y^2 - (\omega^2/c^2)\epsilon_v$, the curve itself gives the lines $\alpha_1 = 0$ in the $\omega - cq_y$ plane. The singularities of ϵ_v occur at $\omega = \omega_T$, where $\epsilon_L(\omega)$ diverges, and at $\omega = \omega_{\pm}$, the two zeros of $\epsilon_{zz}(\omega)$. In the shaded regions, α_1^2 is negative; these correspond to the shaded regions of Fig. 2. Because ϵ_v is a multiple-valued function of ω , it is not surprising that we find additional branches of

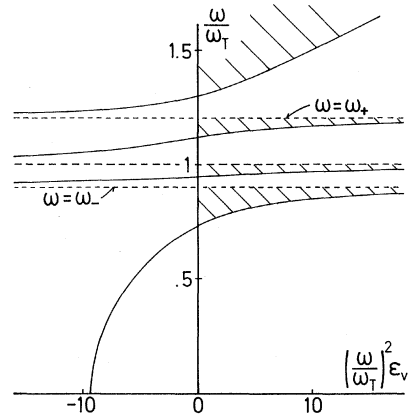


FIG. 3. A plot of $(\omega/\omega_T)^2 \epsilon_v$ versus ω/ω_T for the same set of parameters used in Fig. 2. The function $\epsilon_v(\omega)$ has singularities at $\omega = \omega_T$ and at $\omega = \omega_{\pm}$, where

$$\omega_{\pm}^2 = \frac{1}{2} (\epsilon_0 \epsilon_{\infty}^{-1} \omega_T^2 + \epsilon_{\infty}^{-1} \omega_p^2 + \omega_c^2) \pm \frac{1}{2} \times [(\epsilon_0 \epsilon_{\infty}^{-1} \omega_T^2 + \epsilon_{\infty}^{-1} \omega_p^2 + \omega_c^2)^2 - 4\omega_T^2 (\omega_p^2 + \epsilon_0 \omega_c^2) / \epsilon_{\infty}]^{1/2}$$

are the zeros of ϵ_{zz} . The shaded regions correspond to the shaded regions of Fig. 2, in which α_1^2 is negative.

the dispersion curves (for $q_y < 0$) and regions in which more than two solutions occur for a given value of q_y .

The observation of the multiple-valued dispersion curves shown in Fig. 2 should be an interesting challenge to experimentalists.

The authors would like to thank Professor E. Burstein for sending them a preprint of Ref. 3 prior to publication.

*Work supported in part by the National Science Foundation and the Advanced Research Projects Agency.

†NATO Postdoctoral Fellow. Permanent address: Brown University, Providence, R. I. 02912.

¹K. W. Chiu and J. J. Quinn, *Nuovo Cimento* **10**, 1 (1972).

²K. W. Chiu and J. J. Quinn, *Phys. Rev. B* **5**, 4707 (1972).

³J. J. Brion, R. F. Wallis, A. Hartstein, and E. Burstein, *Phys. Rev. Lett.* **28**, 1455 (1972).

⁴K. W. Chiu and J. J. Quinn, *Phys. Lett.* **35A**, 469 (1971).

⁵W. E. Anderson, R. W. Alexander, and R. J. Bell. *Phys. Rev. Lett.* **27**, 1057 (1971); I. I. Reschina, Yu. M. Gerbstein, and D. I. Mirilin, *Fiz. Tverd. Tela* **14**, 1280 (1972).

⁶The boundary conditions are the continuity of the

tangential components of \vec{E} and \vec{H} . The waves in each medium are of the form $A_i \exp(+|\alpha_i|z) + B_i \exp(-|\alpha_i|z)$. For the semi-infinite media considered here the coefficient of the exponentially growing wave must be

taken to be zero. The dispersion relation (4) is obtained for the polarization whose field is in the y - z plane. This polarization is the only one considered throughout this paper.

Phonon Emission from Terbium Films at 15 GHz*

Michael T. Elliott† and Howard A. Blackstead

Department of Physics, University of Notre Dame, Notre Dame, Indiana 46556

(Received 4 May 1972)

Using a tunable phonon spectrometer, we have observed phonon emission from films of terbium at 1.6°K. The phonon frequency, 15.15 GHz, was found to be the same as the frequency of an rf magnetic field applied parallel to the surface of the film. This observation provides direct support for the so-called free-lattice model of dynamic magnetoelastic coupling in rare-earth metals.

It is well known that the static properties of several of the heavy rare-earth metals are strongly influenced by the existence of large magnetoelastic interactions.¹⁻⁴ Since the magnetoelastic terms in the Hamiltonian involve the coupling of the spins to the lattice, it is to be expected that the dynamic properties, e.g., spin-wave excitations, will be strongly affected. There has been considerable discussion in the literature⁵ relating to how the magnetoelastic terms are to be treated, and a brief review seems appropriate.

Turov and Shavrov⁶ considered the magnetoelastic influence on spin waves by assuming that the lattice remains stationary, or frozen, as the spins precess and they showed that, as a result of the interaction, the spin-wave energy gap would be raised. Cooper^{3,5} evaluated an opposite limit which has become known as the free-lattice model. By allowing the lattice to deform with the spins' motion, he found that the energy gap would be due entirely to anisotropy. Brooks⁷ suggested that for frequencies less than 40 GHz the free-lattice model would apply, but at higher frequencies the strains would be unable to follow the spins' motion, and so the frozen-lattice model would be correct.

Vigren and Liu,⁸ using a microscopic model which allows the spins to couple to localized lattice distortions, showed that at low temperatures and frequencies, for $q \approx 0$, the free-lattice mode could be observed. At higher frequencies, particularly for finite q , the local strains cancel, leaving only the equilibrium strains, and so the frozen lattice results. Their calculations showed a discontinuity in the spin-wave spectrum which resulted from the vanishing of the magnetoelastic

contribution for $q = 0$. They argued that, for a sample of finite size, the spin-wave spectrum would not exhibit a discontinuity, but would vary smoothly depending on the sample size, and therefore allow observation of the free-lattice mode for small q .

Hart and Stanford⁹ studied ferromagnetic resonance in terbium at 24 GHz, and their results agree with the free-lattice model for low frequencies. In earlier work on terbium at 100 GHz, Wagner and Stanford¹⁰ confirmed the frozen-lattice model at high frequencies.

The fundamental assumption of the free-lattice model is that the lattice maintains instantaneous equilibrium with the spins, and it follows that if the spins (magnetization) can be made to precess, phonons will be produced. This results from the fact that for a single crystal, the equilibrium symmetry strains depend on the direction cosines of the magnetization.

Consider a single crystal of terbium with its c and b axes parallel to the y and z directions, respectively (Tb is hcp). With the application of a static magnetic field along the z axis, a magnetically easy direction, and an rf field along the x axis, precession of the magnetization about the z axis at the rf frequency ω results. Unless the conditions for resonance are satisfied, θ (the polar angle measured with respect to the z axis) will be small. In addition, the precession will not be in phase with the rf field, so φ (the azimuthal angle measured with respect to the x axis) will be given by $\varphi = \omega t + \delta$. Here δ is an arbitrary phase which can be neglected for this analysis.

With the use of the results obtained by Callen and Callen,¹¹ transformed to this coordinate sys-